

Electronic Supplementary Material (ESI) for Rsc advances. This journal  
is © The Royal Society of Chemistry 2021

## Supporting Information

### **Hydrazone connected stable luminescent Covalent Organic Polymer for ultrafast detection of nitro-explosives**

Muhammad Asad<sup>a</sup>, Ya-Jie Wang<sup>a</sup>, Shan Wang<sup>a\*</sup>, Qian-You Wang<sup>a</sup>, Lin-Ke Li<sup>a\*</sup>, Qing-Guo  
Dong<sup>a</sup>, Saadat Majeed<sup>b</sup>, Shuang-Quan Zang<sup>a\*</sup>

*<sup>a</sup> Henan Key Laboratory of Crystalline Molecular Functional Materials, Henan International  
Joint Laboratory of Tumor Theranostical Cluster Materials, Green Catalysis Center, and  
College of Chemistry, Zhengzhou University, Zhengzhou 450001, P. R. China*

*<sup>b</sup> Institute of Chemical Sciences, Bahauddin Zakariya University, Multan, 60800, Pakistan*

## Table of contents

Section	Detail	Page.no
i	PXRD spectra of <b>H-COP</b> (Fig. S1)	S3
ii	<sup>13</sup> C CP/MAS Solid-state NMR spectrum of <b>H-COP</b> (Fig. S2)	S4
iii	Photo-physical study (Fig. S3)	S5
iv	Luminogenic status (Fig. S4)	S5
v	Chemical stability (Fig. S5)	S6
vi	Thermal stability test of <b>H-COP</b> (TGA) (Fig. S6)	S6
vii	Quenching and LOD calculations for tested nitro explosive analytes (Fig. S7-S10)	S7-S11
viii	Non-explosives analytes quenching behavior (Fig. S11)	S11
ix	Nitro explosive analytes comparison study with reported polymers (Table S1 & S2)	S12-S13
x	TCSPC profile and calculation for average fluorescence lifetime measurement (Fig. S12) & (Table S3)	S14
xi	DFT calculations (Table S4)	S15
xii	References	S15-S16

**i. PXRD spectra of H-COP**

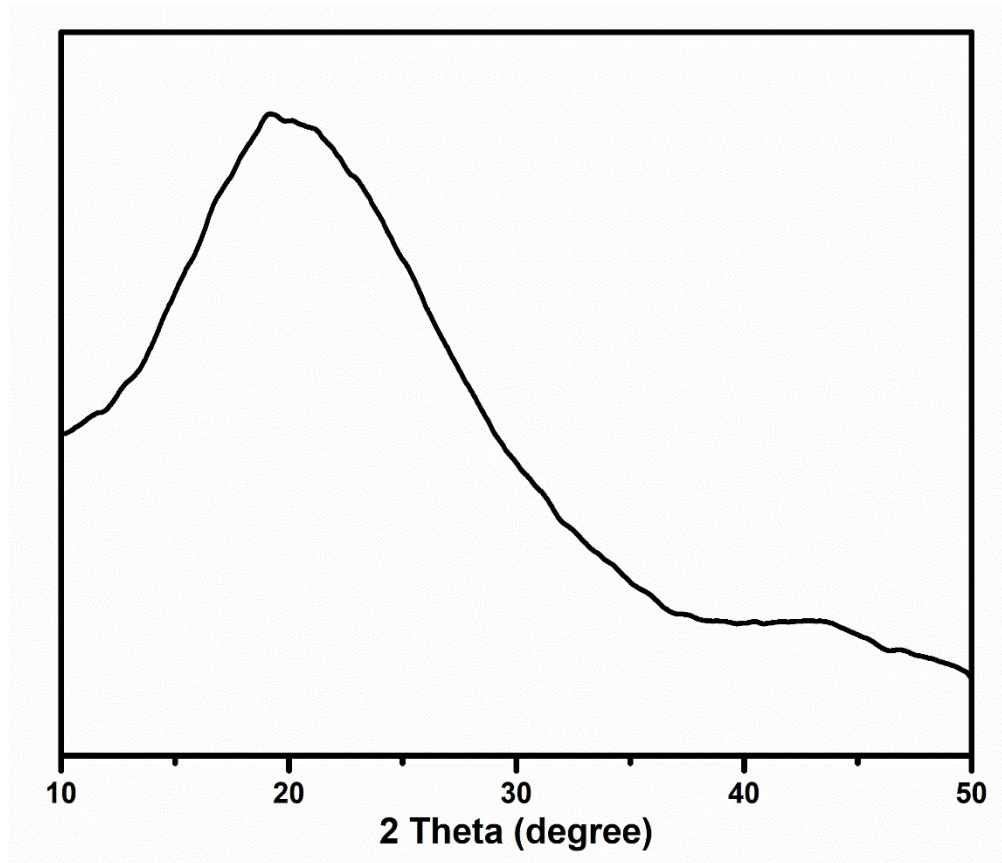


**Fig. S1** PXRD spectra for **H-COP**

ii.  $^{13}\text{C}$  CP/MAS Solid-state NMR spectrum of H-COP

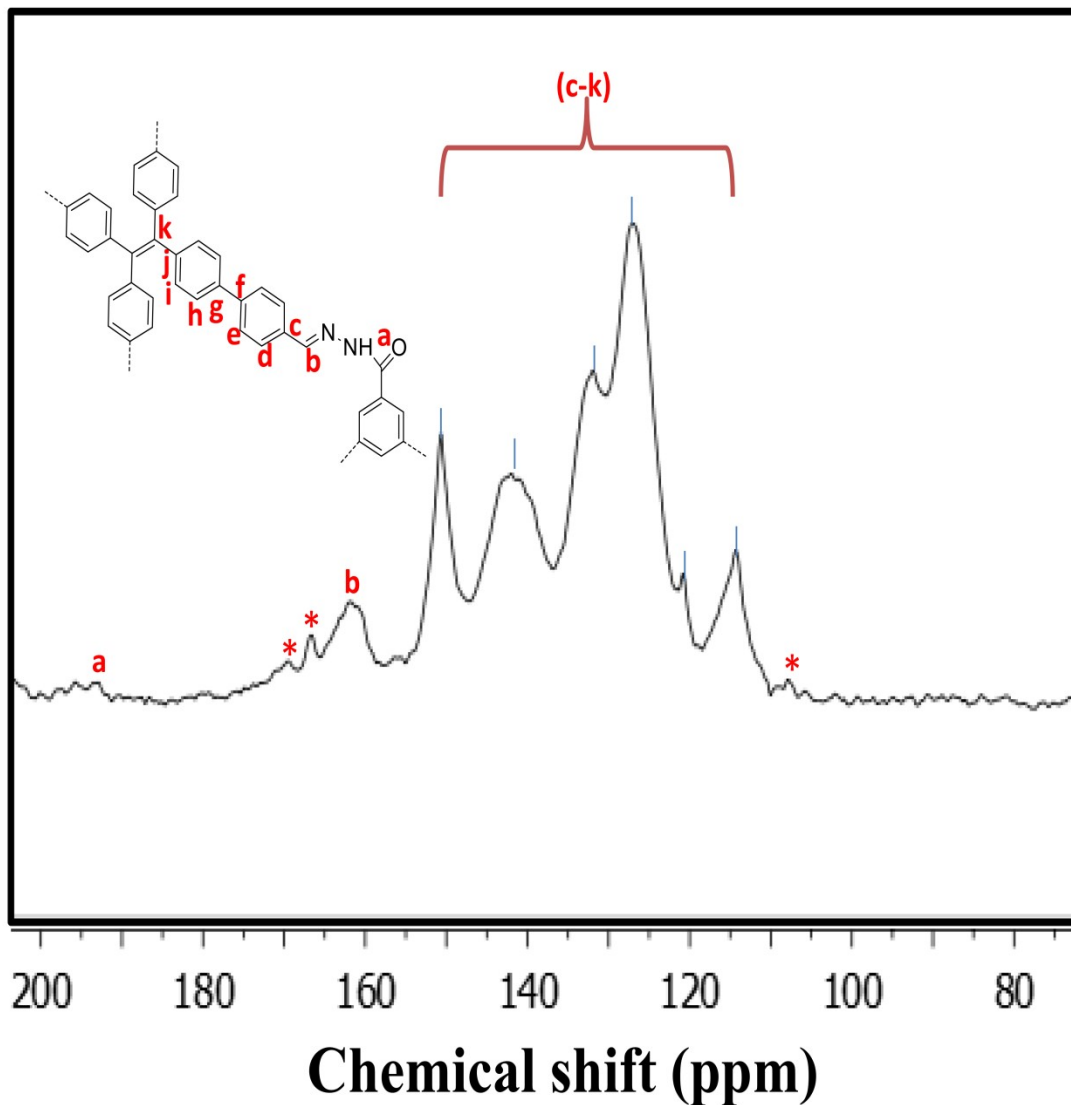


**Fig. S2**  $^{13}\text{C}$  CP/MAS Solid-state NMR spectrum of H-COP: The alphabets (a) represents chemical shift of C=O bond while (b) denotes chemical shift of imine carbon bond around 156 ppm, while Asterisks denote side bands.<sup>1</sup>

### iii. Photo-physical study

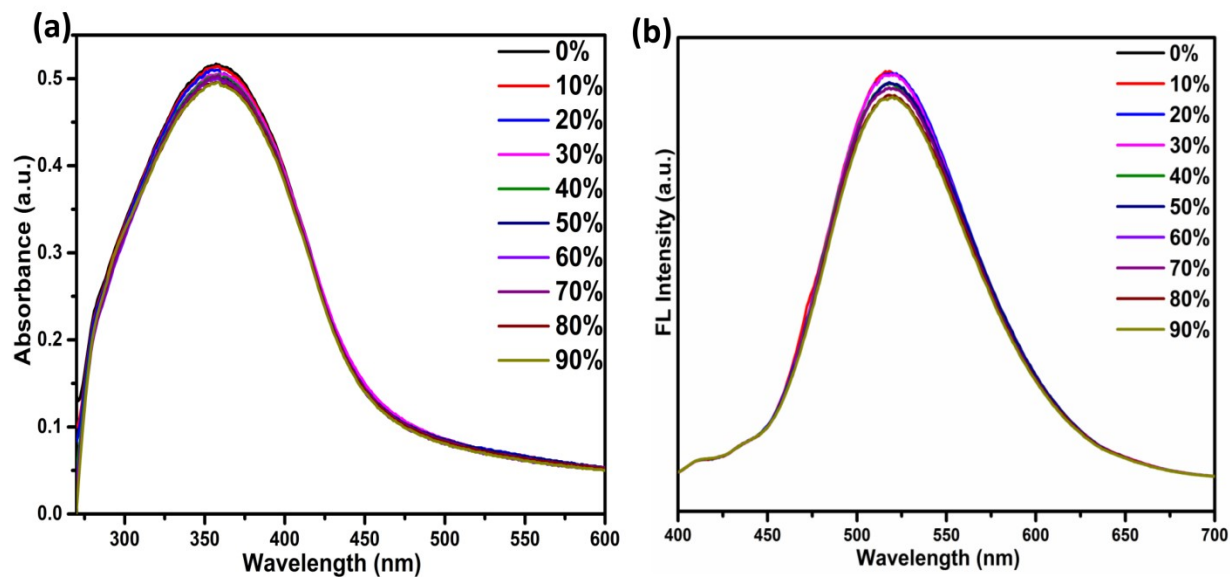


**Fig. S3** UV-vis absorption spectra and emission spectra of **H-COP** dissolving in DMF with a different fraction (0% – 90%) of H<sub>2</sub>O

### iv. Luminogenic status

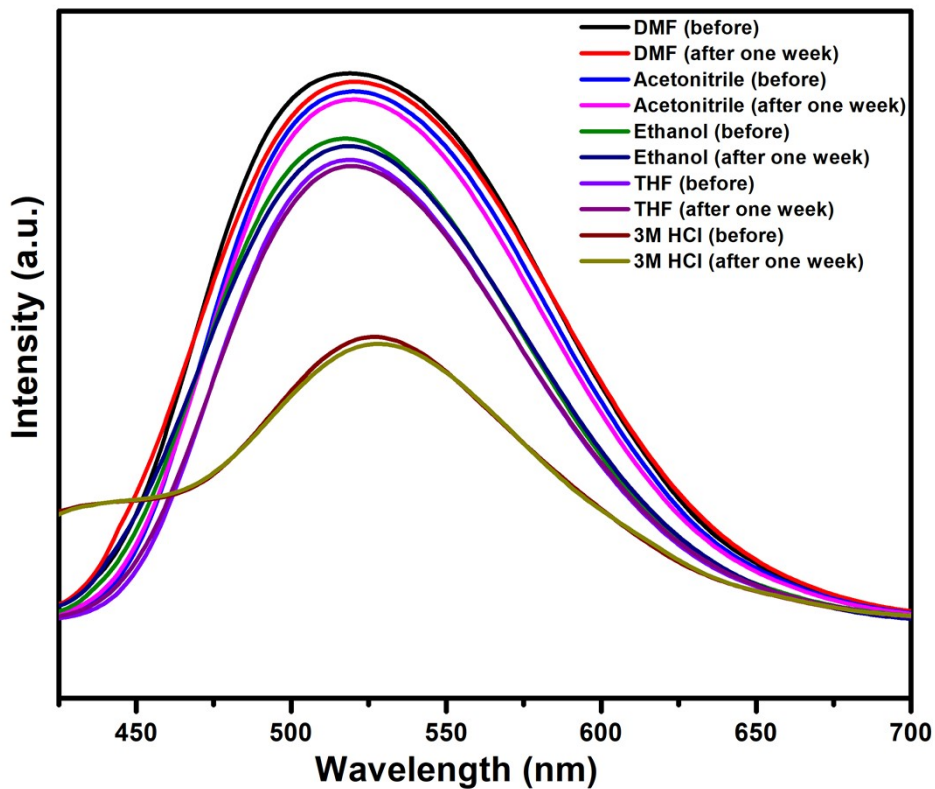


**Fig. S4** Luminogenic status of **H-COP** in different chemical environments after one week

## v. Chemical stability

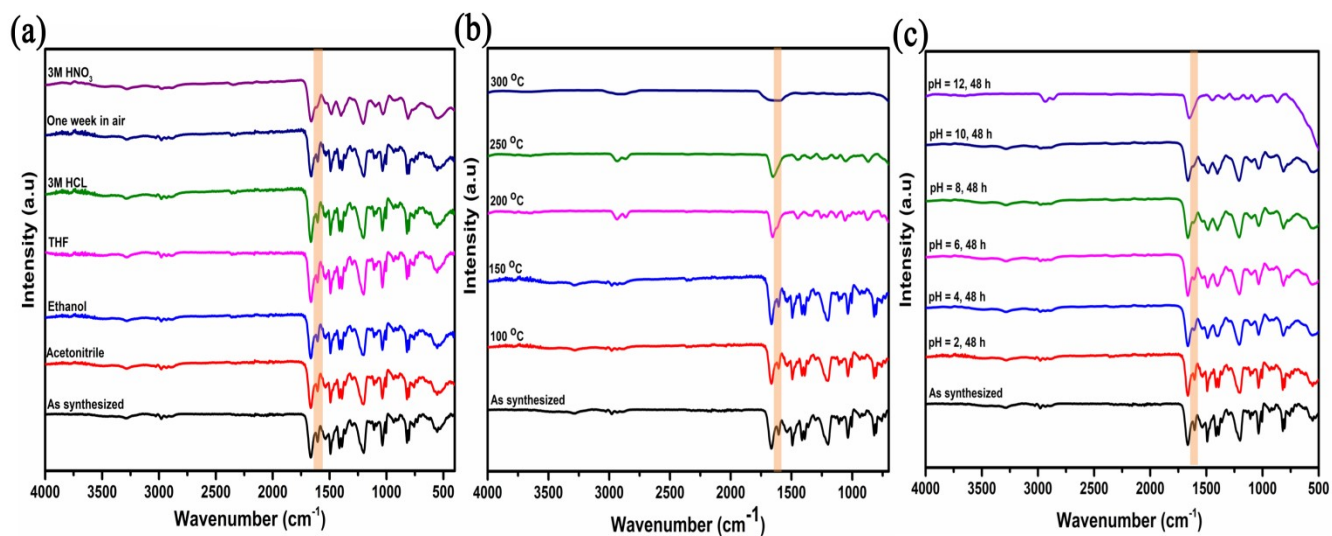


**Fig. S5** The H-COP FTIR spectra after (a) treatment with different chemical environments and (b) heating at different temperatures (c) soaked in different pH

## vi. The thermal stability test of H-COP

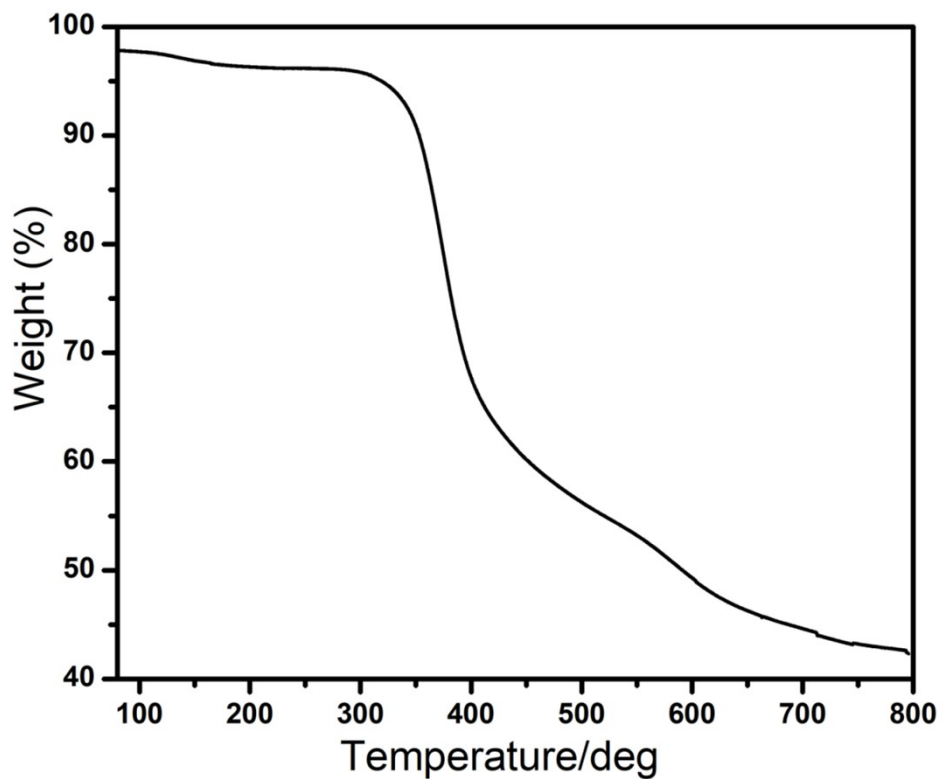


**Fig. S6** The H-COP TGA curve.

**vii. LOD calculations for tested nitro explosive analytes:**

**Standard Deviation ( $\sigma$ ) calculation:**

<b>Blank Readings</b>	<b>FL Intensity</b>
<b>Reading 1</b>	<b>7.86E+06</b>
<b>Reading 2</b>	<b>7.83E+06</b>
<b>Reading 3</b>	<b>7.72E+06</b>
<b>Reading 4</b>	<b>7.28E+06</b>
<b>Reading 5</b>	<b>7.01E+06</b>
<b>Standard Deviation (<math>\sigma</math>)</b>	<b>3.76616E+05</b>

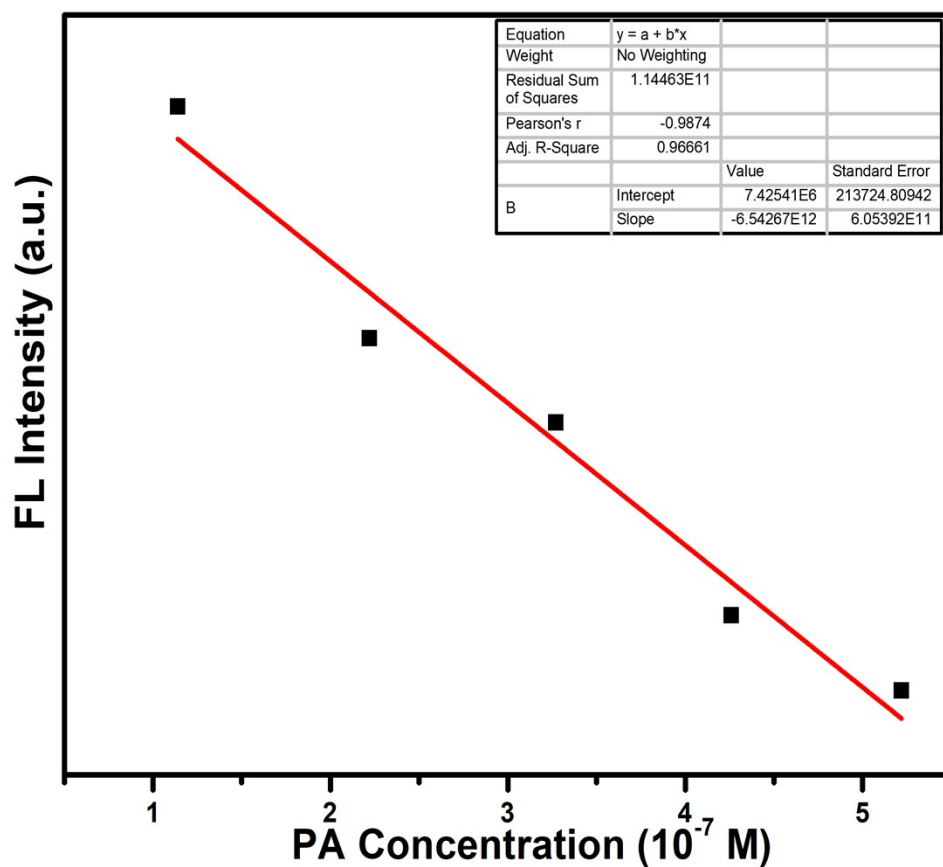


**Fig. S7** Linear region of fluorescence intensity of **H-COP** upon incremental addition of PA at  $\lambda_{em} = 500$  nm (upon  $\lambda_{ex} = 378$  nm) at room temperature.

**Calculation of Detection limit (LOD) for PA:**

Slope (m)	6.5426E+12
Standard deviation ( $\sigma$ )	3.76616E+05
Limit of detection ( $3\sigma/m$ )	0.17 $\mu$ M



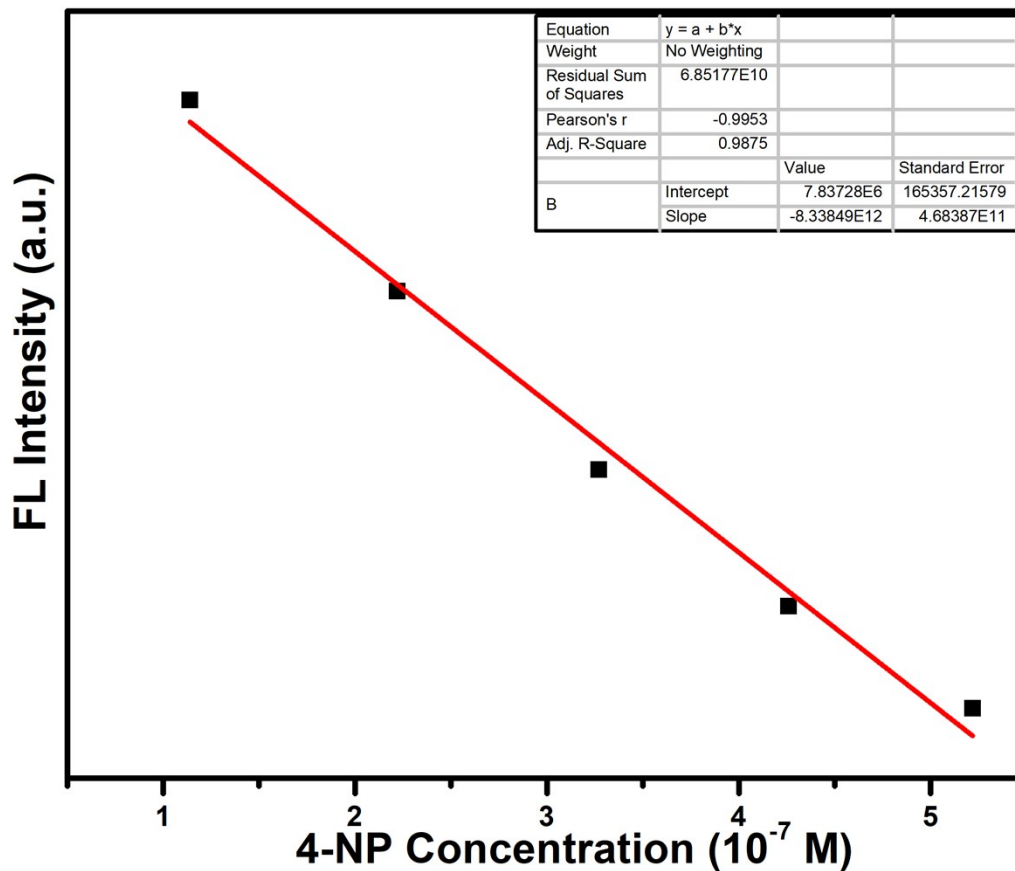


**Fig. S8** Linear region of fluorescence intensity of **H-COP** upon incremental addition of 4-NP at  $\lambda_{em} = 500$  nm (upon  $\lambda_{ex} = 378$  nm) at room temperature.

**Calculation of Detection limit (LOD) for 4-NP:**

Slope (m)	8.33849E+12
Standard deviation ( $\sigma$ )	3.76616E+05
Limit of detection ( $3\sigma/m$ )	0.13 $\mu$ M

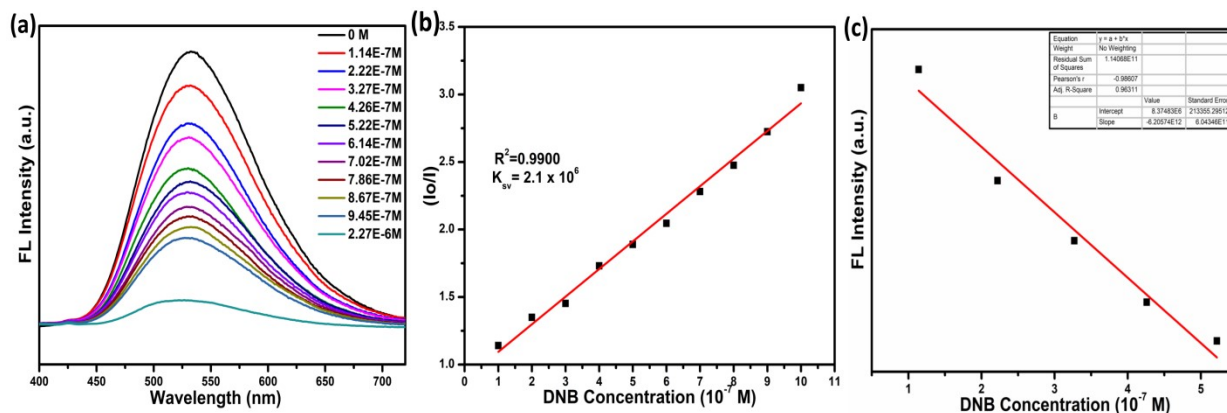


**Fig. S9** Quenching titration graph and LoD calculation for DNB.

**Calculation of Detection limit (LOD) for DNB:**

Slope (m)	6.20574E+12
Standard deviation ( $\sigma$ )	3.76616E+05
Limit of detection ( $3\sigma/m$ )	0.18 $\mu$ M

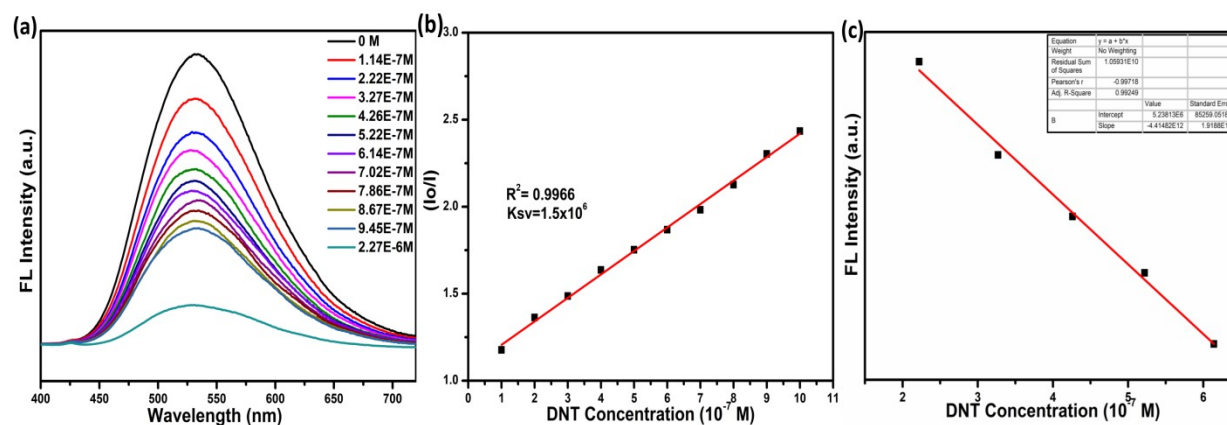


**Fig. S10** Quenching titration graph and LoD calculation for DNT.

**Calculation of Detection limit (LOD) for DNB:**

Slope (m)	4.41482E+12
Standard deviation ( $\sigma$ )	3.76616E+05
Limit of detection ( $3\sigma/m$ )	0.25 $\mu$ M

### viii. Fluorescence quenching pattern of non-explosives analytes

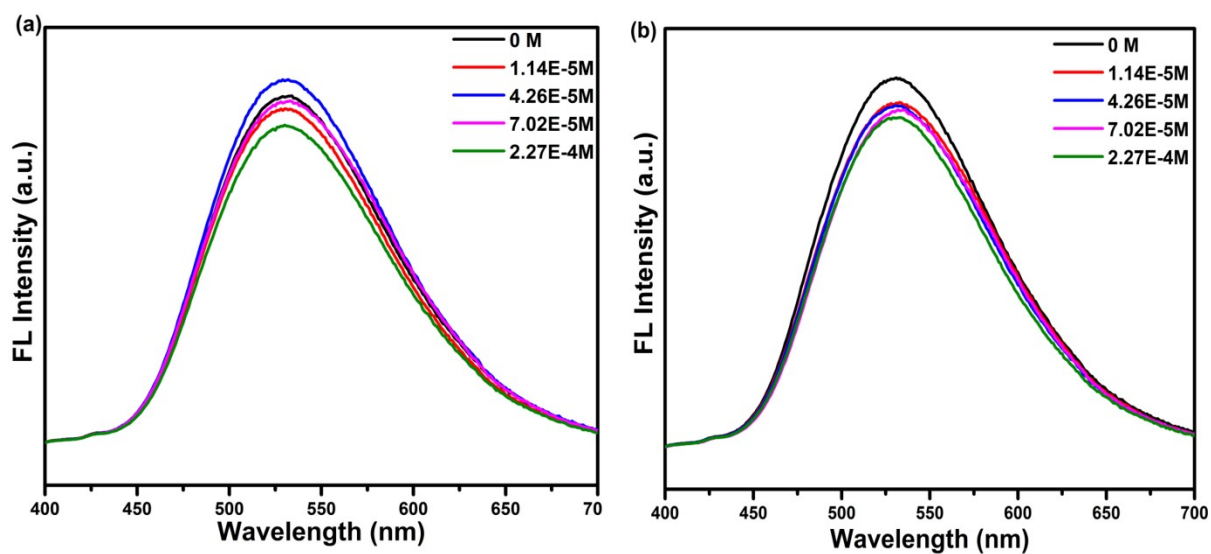


**Fig. S11** Fluorescence quenching pattern for non-explosives analyte (a) Methyl benzene and (b) Dibromobenzene ( $\lambda_{em} = 500$  nm &  $\lambda_{ex} = 378$  nm) at room temperature.

## ix. Comparison study of tested nitro explosive analytes with reported Polymers

Table S1 PA sensing comparison with reported Polymers

Materials	$K_{sv}$	LOD	Medium	Ref.
H-COP	$2.5 \times 10^6 \text{ M}^{-1}$	0.17 $\mu\text{M}$	DMF	This work
$[\text{Tb}_2(\text{PBA})_3(\text{H}_2\text{O})_3 \cdot \text{DMF} \cdot 3\text{H}_2\text{O}]_n$	$4.5 \times 10^4 \text{ L/mol}$	0–30 $\mu\text{mol/L}$	DMF.H <sub>2</sub> O	2
FPP-3	$6020 \text{ M}^{-1}$	13.20 ppb	DMF/K <sub>2</sub> CO <sub>3</sub>	3
PS-OPV-NH <sub>2</sub>	NA	58 nM	H <sub>2</sub> O	4
H-COP-612	$2.51 \times 10^5 \text{ M}^{-1}$	NA	DMF	5
$[\text{Zn}(\mu\text{-HCIP})(\mu\text{-pbix}) \cdot 2\text{H}_2\text{O}]_n$	$4.37 \times 10^4 \text{ M}^{-1}$	56.46 ppb	DMF	6
Cd-based CPs	$96907 \text{ M}^{-1}$	15 ppb	DCM	7
H-COP-301	$2.6 \times 10^5 \text{ M}^{-1}$	1 ppm	Methanol	8
H-COP-401	$8.3 \times 10^4 \text{ M}^{-1}$	1 ppm	Methanol	8
(Ln-CPs)([Eu(L) <sub>2</sub> (H <sub>2</sub> O)]BrH <sub>2</sub> O) <sub>n</sub> (EuBr)	$17000 \text{ M}^{-1}$	10 <sup>-5</sup> M	H <sub>2</sub> O	9
([TbL <sub>2</sub> (H <sub>2</sub> O) <sub>2</sub> ]BrH <sub>2</sub> O) <sub>n</sub> (TbBr)	$20200 \text{ M}^{-1}$	10 <sup>-5</sup> M	H <sub>2</sub> O	9
TBAFP1	$5.3 \times 10^5 \text{ M}^{-1}$	144 nM	THF	10
TBAPF2	$2.4 \times 10^5 \text{ M}^{-1}$	151 nM	THF	10
(Ln-CPs)	$2.6 \times 10^5 \text{ L/mol}$	0.28 $\mu\text{molL}^{-1}$	Ethanol	11
$[\text{Zn}_3(\text{mtrb})_3(\text{btc})_2 \cdot 3\text{H}_2\text{O}]_n$	$3.26 \times 10^4 \text{ M}^{-1}$	0.22 $\mu\text{M}$	Methanol	12

NA= Not available

**Table S2.** 4-NP sensing comparison with reported Polymers

Materials	$K_{Sv}$ ( $M^{-1}$ )	LOD	Medium	Ref.
H-COP	$3.8 \times 10^6$	0.13 $\mu$ M	DMF	This work
(Ln-CPs)	$1.9 \times 10^5$	0.98 $\mu$ M	Ethanol	11
$[Zn_3(mtrb)_3(btc)_2 \cdot 3H_2O]_n$	$1.276 \times 10^4$	NA	Methanol	12
$[Cd_2(obtz)(Meip)_2 \cdot H_2O]_n$	0.0879	$\leq 20$ ppm	Ethanol	13
$[Cd(obtz)(ndc) \cdot 0.5H_2O]_n$	0.0662	$\leq 30$ ppm	Ethanol	13
(BpaD)	NA	0.6 $\mu$ M	(PBS:ethanol=9:1)	14
(BpaP)	NA	0.23 $\mu$ M	(PBS:ethanol=9:1)	14
$[Tb(BTEC)_{0.5}(HCOO)(H_2O)_2]$	$2.04 \times 10^4$	0.46ppm	THF	15
LCP	$3.8 \times 10^4$	$0.49 \times 10^{-3}$ M	H <sub>2</sub> O	16

NA= Not available

**Note:**

PA and 4-NP references are available for comparison with reported luminescent polymer materials. PA comparison table has been shown in original manuscript, while other explosives like DNT, DNB didn't contain enough data for comparison with luminescent polymers. Hence our polymer shows greater selectivity for these explosives among reported polymer materials.

## x. TCSPC profile and calculation for average fluorescence lifetime

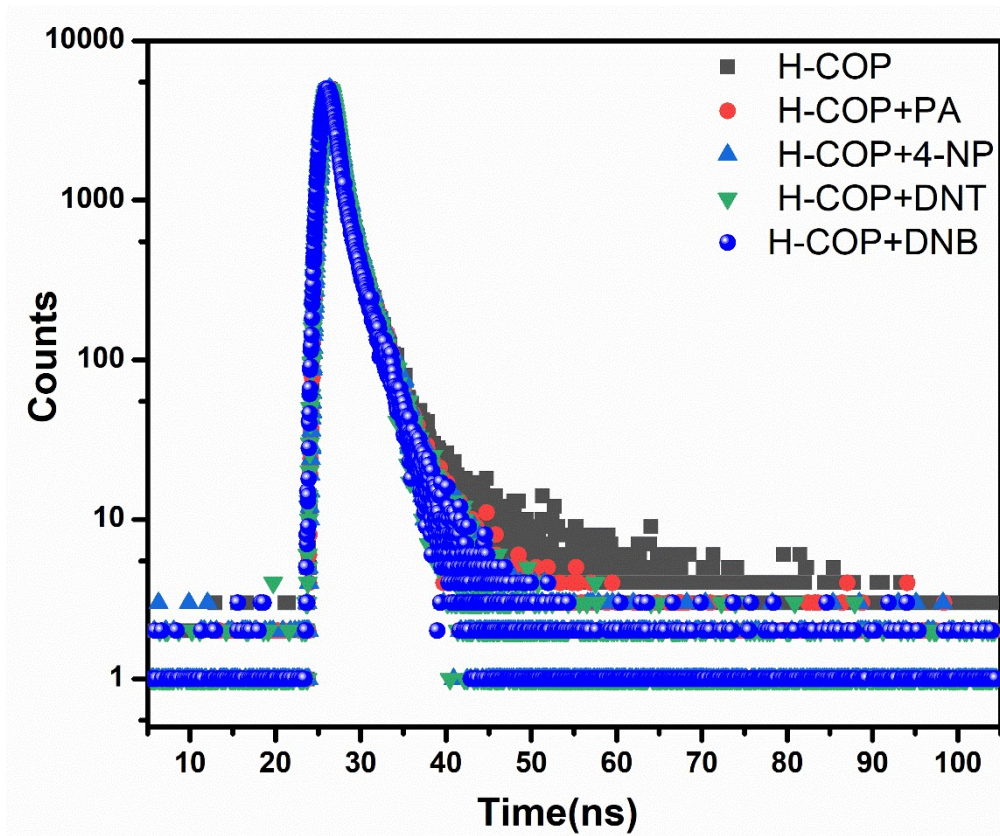


**Fig. S12** The **H-COP** average luminescence lifespan decay profile with different common explosives ( $\lambda_{\text{ex}}=378$  nm &  $\lambda_{\text{em}}=500$  nm).

**Table S3. TCSPC calculation of H-COP and nitro explosives analytes**

Samples	T1 (ns)	T2 (ns)	B1	B2	A1=[B1/SumB]	A2=[B2/SumB]	<I> (ns)
<b>H-COP</b>	1.5649	5.1379	69.50	30.50	0.695	0.305	2.65
<b>H-COP + PA</b>	0.1611	2.1364	5.66	94.34	0.056	0.9434	2.02
<b>H-COP + 4-NP</b>	0.7828	2.5102	40.44	59.59	0.4044	0.5959	1.81
<b>H-COP + DNT</b>	0.8033	2.5831	47.67	52.33	0.4767	0.5233	1.73
<b>H-COP + DNB</b>	0.8779	2.6575	53.64	46.36	0.5364	0.4636	1.72

**xi. Table. S4 DFT calculations using B3LYP/6-31G\*<sup>17</sup>**

Analytes	HOMO (eV)	LUMO (eV)	Band gap (eV)
H-COP	-5.605	-2.35	3.255
PA	-8.4592	-3.4726	4.986
4-NP	-7.577	-2.499	5.078
2,4-DNT	-8.09	-2.97	5.12
1,3-DNB	-8.32	-3.14	5.18

**xii. References**

1. M. Faheem, S. Aziz, X. Jing, T. Ma, J. Du, F. Sun, Y. Tian and G. Zhu, Dual luminescent covalent organic frameworks for nitro-explosive detection. *J. Mat. Chem. A.*, 2019, **7**, 27148-27155.
2. C.-H. Wang, B. Sheng, Z. Zhang, M. Deng, J.-J. Xue and Y.-G. Ma, Luminescent Coordination Polymer for Picric Acid Detection and Treatment on Spinal Cord Injury Model Via Upregulating the trka Expression. *J. Fluorescence.*, 2020, 1-7.
3. R. Sun, S. Feng, B. Zhou, Z. Chen, D. Wang and H. Liu, Flexible Cyclosiloxane-Linked Fluorescent Porous Polymers for Multifunctional Chemical Sensors. *ACS Mac. Lett.*, 2019, **9**, 43-48.
4. S. K. Makkad, Amine decorated polystyrene nanobeads incorporating  $\pi$ -conjugated OPV chromophore for picric acid sensing in water. *RSC Adv.*, 2020, **10**, 6497-6502.
5. L. Guo, D. Cao, J. Yun and X. Zeng, Highly selective detection of picric acid from multicomponent mixtures of nitro explosives by using COP luminescent probe. *Sens. Actuators B Chem.*, 2017, **243**, 753-760.
6. M. r. Arici, Luminescent 2D+ 2D  $\rightarrow$  2D interpenetrated Zn (II)-coordination polymer based on reduced schiff base tricarboxylic acid and bis (imidazole) ligand for detection of picric acid and Fe<sup>3+</sup> ions. *Cryst. Growth Des.*, 2017, **17**, 5499-5505.
7. S. I. Vasylevskiy, D. M. Bassani and K. M. Fromm, Anion-induced structural diversity of Zn and Cd coordination polymers based on bis-9, 10-(pyridine-4-yl)-anthracene, their

- luminescent properties, and highly efficient sensing of nitro derivatives and herbicides. *Inorg. Chem.*, 2019, **58**, 5646-5653.
8. N. Sang, C. Zhan and D. Cao, Highly sensitive and selective detection of 2, 4, 6-trinitrophenol using covalent-organic polymer luminescent probes. *J. Mat. Chem. A.*, 2015, **3**, 92-96.
  9. C. Xu, H. Huang, J. Ma, W. Liu, C. Chen, X. Huang, L. Yang, F.-X. Pan and W. Liu, Lanthanide (iii) coordination polymers for luminescence detection of Fe (iii) and picric acid. *New. J. Chem.* 2018, **42**, 15306-15310.
  10. M. Ansari, R. Bera, S. Mondal and N. Das, Triptycene-derived photoresponsive fluorescent azo-polymer as chemosensor for picric acid detection. *ACS Omega.*, 2019, **4**, 9383-9392.
  11. X. Shi, X. Qu, J. Chai, C. Tong, Y. Fan and L. Wang, Stable coordination polymers with linear dependence color tuning and luminescent properties for detection of metal ions and explosives. *Dyes. and Pigm.*, 2019, **170**, 107583.
  12. Y.-Q. Zhang, V. A. Blatov, T.-R. Zheng, C.-H. Yang, L.-L. Qian, K. Li, B.-L. Li and B. Wu, A luminescent zinc (II) coordination polymer with unusual (3, 4, 4)-coordinated self-catenated 3D network for selective detection of nitroaromatics and ferric and chromate ions: a versatile luminescent sensor. *Dalt.Trans.*, 2018, **47**, 6189-6198.
  13. S. Zhao, J.-G. Ding, T.-R. Zheng, K. Li, B.-L. Li and B. Wu, The 3D and 2D cadmium coordination polymers as luminescent sensors for detection of nitroaromatics. *J.Luminescen.*, 2017, **188**, 356-364.
  14. X. Wang, Y. Zuo and S. Feng, Ultrasensitive polysiloxane-based fluorescent probes for selectively detecting of 4-nitrophenol and their application in paper sensors. *Mat.Tod. Comm.*, 2020, **25**, 101570.
  15. R. F. Bogale, Y. Chen, J. Ye, Y. Yang, A. Rauf, L. Duan, P. Tian and G. Ning, Highly selective and sensitive detection of 4-nitrophenol and Fe<sup>3+</sup> ion based on a luminescent layered terbium (III) coordination polymer. *Sens. Actuators B Chem.*, 2017, **245**, 171-178.
  16. J. Zhang, L. Gao, Y. Wang, L. Zhai, X. Niu and T. Hu, A novel 3D Cd-based luminescent coordination polymer for selective sensing of 4-NP and NZF. *New.J. Chem.*, 2019, **43**, 16853-16859.
  17. H. Kruse, L. Goerigk and S. J. T. J. o. o. c. Grimme, Why the standard B3LYP/6-31G\* model chemistry should not be used in DFT calculations of molecular thermochemistry: understanding and correcting the problem. *J. Org. Chem.*, 2012, **77**, 10824-10834.